Provided for non-commercial research and education use.
Not for reproduction, distribution or commercial use.

(This is a sample cover image for this issue. The actual cover is not yet available at this time.)

This article appeared in a journal published by Elsevier. The attached copy is furnished to the author for internal non-commercial research and education use, including for instruction at the authors institution and sharing with colleagues.

Other uses, including reproduction and distribution, or selling or licensing copies, or posting to personal, institutional or third party websites are prohibited.

In most cases authors are permitted to post their version of the article (e.g. in Word or Tex form) to their personal website or institutional repository. Authors requiring further information regarding Elsevier's archiving and manuscript policies are encouraged to visit:

http://www.elsevier.com/copyright

Author's personal copy

International Journal of Greenhouse Gas Control 6 (2012) 230–245

Contents lists available at SciVerse ScienceDirect

International Journal of Greenhouse Gas Control

journal homepage: www.elsevier.com/locate/ijggc

Active CO_2 reservoir management for carbon storage: Analysis of operational strategies to relieve pressure buildup and improve injectivity

Thomas A. Buscheck[a,*], Yunwei Sun[a], Mingjie Chen[a], Yue Hao[a], Thomas J. Wolery[a], William L. Bourcier[a], Benjamin Court[b], Michael A. Celia[b], S. Julio Friedmann[a], Roger D. Aines[a]

[a] Lawrence Livermore National Laboratory, P.O. Box 808, Livermore, CA 94550, USA
[b] Department of Civil and Environmental Engineering, Princeton University, Princeton, NJ 08544, USA

ARTICLE INFO

Article history:
Received 29 May 2011
Received in revised form 9 November 2011
Accepted 10 November 2011

Keywords:
CO_2 capture and storage
CO_2 capture
Utilization and storage
Brine production
Pressure management
Injectivity
CO_2 migration

ABSTRACT

For industrial-scale CO_2 injection in saline formations, pressure buildup can limit storage capacity and security. Active CO_2 Reservoir Management (ACRM) combines brine production with CO_2 injection to relieve pressure buildup, increase injectivity, manipulate CO_2 migration, and constrain brine leakage. By limiting pressure buildup, in magnitude, spatial extent, and duration, ACRM can reduce CO_2 and brine leakage, minimize interactions with neighboring subsurface activities, allowing independent assessment and permitting, reduce the Area of Review and required duration of post-injection monitoring, and reduce cost and risk. ACRM provides benefits to reservoir management at the cost of extracting brine. The added cost must be offset by the added benefits to the storage operation and/or by creating new, valuable uses that can reduce the total added cost. Actual net cost is expected to be site specific, requiring detailed analysis that is beyond the scope of this paper, which focuses on the benefits to reservoir management. We investigate operational strategies for achieving an effective tradeoff between pressure relief/improved-injectivity and delayed CO_2 breakthrough at brine producers. For vertical wells, an injection-only strategy is compared to a pressure-management strategy with brine production from a double-ring 9-spot pattern. Brine production allows injection to be steadily ramped up while staying within the pressure-buildup target, while injection-only requires a gradual ramp-down. Injector/producer horizontal-well pairs were analyzed for a range of well spacings, storage-formation thickness and area, level and dipping formations, and for homogeneous and heterogeneous permeability. When the producer is downdip of the injector, the combined influence of buoyancy and heterogeneity can delay CO_2 breakthrough. Both vertical and horizontal wells can achieve pressure relief and improved CO_2 injectivity, while delaying CO_2 breakthrough. Pressure buildup and CO_2 breakthrough are sensitive to storage-formation permeability and insensitive to all other hydrologic parameters except caprock-seal permeability, which only affects pressure buildup for injection-only cases.

© 2011 Elsevier Ltd. All rights reserved.

1. Introduction

In order to stabilize atmospheric CO_2 concentrations for climate change mitigation, CO_2 capture and storage (CCS) implementation must be increased by several orders of magnitude over the next two decades (Fig. 3 of IEA, 2009). CCS in deep geological formations is regarded as a promising means of lowering the amount of CO_2 emitted to the atmosphere and thereby mitigate global climate change (IEA, 2007). In order for widespread deployment of industrial-scale CCS to be achievable, a number of implementation barriers must be addressed. Previously identified barriers, such as CO_2 capture cost, absence of CO_2 transport network, sequestration safety, legal and regulatory barriers, and public acceptance have been recognized for a number of years, as discussed in the Special Report on CCS (SRCCS) (IPCC, 2005). Implementation barriers receiving more recent attention include water-use demands from CCS operations and pore-space competition with emerging activities, such as shale-gas production (Court et al., 2011a). The implementation barrier of water-use demands for CCS may be particularly acute in regions where water resources are already scarce. A comprehensive review is presented by Court et al. (2011a) of progress, since the SRCCS, on several of these large-scale CCS implementation challenges: water, sequestration, and pore-space competition; legal and regulatory; and public acceptance.

Active CO_2 Reservoir Management (ACRM), in conjunction with CO_2 Capture, Utilization, and Storage (CCUS), is being considered as a means of addressing some of these implementation barriers

* Corresponding author at: Lawrence Livermore National Laboratory, P.O. Box 808, L-223, Livermore, CA 94551, USA. Tel.: +1 925 423 9390; fax: +1 925 423 0153.
E-mail address: buscheck1@llnl.gov (T.A. Buscheck).

1750-5836/$ – see front matter © 2011 Elsevier Ltd. All rights reserved.
doi:10.1016/j.ijggc.2011.11.007

Author's personal copy

(Buscheck et al., 2011a,b,c; Court et al., 2011a,b; Court, 2011). In this paper, we first discuss the challenges of saline-formation CCS in Section 1.1. We then suggest potential operational and licensing benefits of ACRM in Section 1.2, and how brine produced by ACRM may enable utilization aspects of CCUS in Section 1.3. In Sections 2 and 3, we examine how ACRM may enhance CO_2 storage, through an analysis of operational strategies to manipulate CO_2 migration, relieve reservoir pressure buildup, and improve injectivity, while delaying the breakthrough of CO_2 at brine producers.

1.1. Background

The most promising settings for widespread deployment of industrial-scale CCS are depleted oil reservoirs, particularly those suited to CO_2-based Enhanced Oil Recovery (CO_2-EOR), and deep saline formations, with each having the advantage of being well separated from the atmosphere. Industrial-scale CO_2 storage will involve large volumes of injected fluid and a need for significant formation storage capacity (Buscheck et al., 2011c). A distinct advantage of CO_2-EOR is that it involves fluid production (i.e., extraction), which increases CO_2 storage capacity and relieves pressure buildup, while injection-only, saline-formation CCS does not (Buscheck et al., 2011c). Yet, because of limitations in the volume and distribution of depleted oil reservoirs and the large volumes and widespread availability of saline formations, CO_2 storage in saline formations is likely to play a more dominant role in CCS (IPCC, 2005). The absence of fluid production in injection-only, industrial-scale, saline-formation CCS may result in a large pressure buildup, particularly in closed or semi-closed formations, persisting both during and long after injection has ceased. Such large and lasting pressure perturbations will require careful monitoring and may require restriction of injection pressures to prevent increasing "failure" risks of caprock fracturing, leakage up abandoned wells, and induced seismicity (Morris et al., 2011; Rutqvist et al., 2007; Bachu, 2008). If not sufficiently controlled, high pressures may drive CO_2 and brines through leakage pathways and threaten water quality in shallower water-supply aquifers (Bachu, 2008; Carroll et al., 2008). Thus, pressure buildup is considered to be a limiting factor on CO_2 storage capacity and security, and storage-capacity estimates based on effective pore volume available for safe trapping of CO_2 may have to be substantially reduced (Birkholzer and Zhou, 2009). A basin-scale reservoir model showed large enough pressure interference between neighboring CCS operations to suggest that the potential area to be characterized in a CCS permitting process, including the Area of Review (AoR), could be quite large, and preclude the possibility of permits being granted on a single-site basis alone (Birkholzer and Zhou, 2009).

1.2. Active CO_2 Reservoir Management (ACRM)

Active CO_2 Reservoir Management (ACRM) is being developed to enable CO_2 Capture, Utilization, and Storage (CCUS) in saline formations. ACRM combines brine production with CO_2 injection (Buscheck et al., 2011c; Court et al., 2011a,b) with the primary goal of enhancing reservoir performance, thereby enabling more secure and cost-effective CO_2 storage. The specific reservoir performance objectives of ACRM are to relieve pressure buildup, increase CO_2 injectivity, increase available pore space and storage capacity, manipulate CO_2 migration, and constrain brine migration. ACRM is being considered for specific CCS sites in the state of Wyoming (Surdam et al., 2009) and off the coast of Norway (Bergmo et al., 2011). ACRM practice is inherent to all CO_2-EOR operations. Because CO_2-EOR utilizes CO_2 in a beneficial fashion, it is a CCUS process. ACRM provides an opportunity to pursue a second goal, developing potential utilization options for produced brine (Buscheck et al., 2011a,b).

ACRM has the potential of providing reservoir performance advantages for CO_2-storage-formation siting, site characterization, model calibration, uncertainty reduction, and permitting. Compared to injection-only CCS, ACRM enables greater control of subsurface fluid migration and pressure perturbations. Brine production allows for "push–pull" manipulation of the CO_2 plume, which can expose *less* of the caprock seal to CO_2 and *more* of the storage formation to CO_2, with a greater fraction of the storage formation utilized for trapping mechanisms (Buscheck et al., 2011c). Another form of CO_2 plume manipulation involves reinjection of brine on top of the CO_2 plume to accelerate CO_2 dissolution and increase solubility trapping (Keith et al., 2004; Hassanzadeh et al., 2009).

When CO_2-storage capacity is increased and brine migration reduced, the area required for securing mineral rights is reduced per unit of stored CO_2. If the net extracted volume of brine is equal to the injected CO_2 volume, pressure buildup and the areal extent of pressure perturbations are minimized, reducing the Area of Review (AoR) by as much as two orders of magnitude (Buscheck et al., 2011c). Definition and determination of the AoR is presented in Court (2011). Their work demonstrated the potential of AoR reduction from brine production using a simple analytical model (Court, 2011). Court (2011) also provide a reservoir-scale quantification of the reduction of CO_2 and brine leakage through thousands of abandoned wells, resulting from pressure relief caused by brine production. ACRM has the potential of reducing other risks associated with pressure buildup, such as induced seismicity. ACRM also has the potential of reducing the volume of rock over which brine may migrate by more than two orders of magnitude (Buscheck et al., 2011c).

Brine producers can function as actively controlled monitoring wells, providing valuable information about CO_2-plume migration when CO_2 breakthrough occurs, which supports history matching and model calibration and also reduces uncertainty. The use of "smart-well" technology, with down-hole sensors and multiple independently controlled production zones (Brouwer et al., 2001; Brouwer and Jansen, 2004; Sudaryanto and Yortsos, 2001; Alhuthali et al., 2007), could extend the useful lifetime of a brine producer beyond when CO_2 is first detected. Down-hole zonal control could also be applied to CO_2 injectors, which would further enhance the ability to manipulate the CO_2 plume. After CO_2 breakthrough can no longer be mitigated by zonal control, it could be possible to convert a brine producer to a CO_2 injector, which would increase overall CO_2 injectivity and facilitate additional zonal control of CO_2-plume migration.

Reducing the areal and vertical extent of pressure perturbations and fluid migration would lessen the possibility of imposing operational constraints on adjacent subsurface activities, including neighboring CCS operations. Minimized pressure and fluid-migration interactions between neighboring CCS operations facilitates independent planning, assessment, and permitting of each CCS operation within a basin. It would also reduce pore-space competition with other subsurface activities, such as shale-gas, deep liquid-waste injection, and geothermal energy production. Thus, ACRM could allow CCS sites to operate in closer proximity to other subsurface activities than possible for injection-only CCS operations. These benefits can help streamline permitting.

In this study we assume an extraction ratio of one, which is a volumetric balance between injected CO_2 and the net extraction (extraction minus reinjection) of brine. It is important to note that this is just one end member of ACRM, which can also involve extraction ratios less than one. Depending on storage-formation depth, an extraction ratio of one requires the removal of between 1.25 and 1.5 m^3 of brine per ton of injected CO_2. For a 1 GWe coal plant this would require the net removal of about 10–12 million m^3 (8100–9700 acre feet) of brine per year from the storage formation.

Author's personal copy

Therefore, a major challenge for ACRM is developing cost-effective solutions to reducing the volume of brine in the storage formation, which is discussed in the next section.

1.3. CO_2 Capture, Utilization, and Storage (CCUS)

ACRM provides benefits to reservoir management at the cost of extracting brine. This added cost must be offset by the added benefits to the storage operation (e.g., fewer injection wells, reduced CO_2 compression cost, smaller AoR, and reduced duration of monitoring) and/or by creating new, valuable uses that can reduce the total added cost. Utilization options of choice for a particular CCUS site depend on the chemical composition and temperature of the produced brine, as well as the proximity to the potential markets. Useful products may include freshwater, saline cooling water, make-up water for oil, gas, and geothermal energy production, and direct recovery of geothermal energy (Harto and Veil, 2011; Bourcier et al., 2011; Buscheck, 2010; Buscheck et al., 2011b). Because brine disposal is a major challenge for ACRM, a key objective for brine utilization is to provide environmentally safe, cost-effective solutions for brine disposition. Because of its importance to the viability of ACRM, we present an overview of potential brine utilization/disposition options.

Brine-utilization options involve a full range of treatment possibilities, from desalination to produce freshwater, to softening (e.g., ion exchange or nanofiltration) and/or the addition of corrosion inhibitors to produce saline cooling water for power plants, to possibly no treatment for make-up water that is injected for pressure support in oil, gas, and geothermal energy production. When it is feasible to use brine as make-up water there is no brine disposal issue. When brine is used as a feedstock to produce freshwater or for saline cooling water, there is the need to either dispose of or to reinject the residual brine, either into the CO_2 storage formation itself or into a separate formation.

The net volume of produced brine can be reduced by partial treatment to yield freshwater along with more concentrated brine which is returned to the reservoir with net volume reduction. While this may be the most valuable option, on a per unit basis, it also involves the most expensive forms of brine treatment because it requires desalination, such as Reverse Osmosis (RO). Produced brine can also be used for cooling purposes, such as in saltwater or brackish-water cooling towers (Maulbetsch and DiFilippo, 2010), with cooling water blowdown (concentrated residual brine) either disposed of or returned to the reservoir. Compared to desalination, this option requires less-costly treatment, such as softening by ion exchange or nanofiltration and/or the addition of corrosion inhibitors (Duke, 2007). Evaporation is inherent to utilizing water for cooling purposes. The benefit of using brine for cooling is to supplant the need to consume valuable freshwater resources by evaporation during the cooling process. For ACRM, the benefit of evaporation is that it reduces the volume of residual brine. An important consideration in the feasibility of utilizing brine for cooling purposes is the cost of brine transportation between the CO_2-storage formation and cooling-water user (Harto and Veil, 2011).

Bourcier et al. (2011) conducted a preliminary cost estimate for RO desalination of produced brine associated with CO_2 storage. They found current RO technology capable of treating salinities up to about 85,000 mg/L TDS (total dissolved solids), which is a value not exceeded in about half of the sampled formation brines in the United States (Aines et al., 2011; based on data from Breit, 2002). For fresh water production, Bourcier et al. (2011) estimated RO desalination costs ranging from \$0.32 to \$0.80/m^3 of permeate (fresh water). Their estimates included costs of all surface facilities, transfer pumps, heat exchangers for cooling, and piping, but did not include the cost of brine production and reinjection wells, which will be site dependent. For a net removal of 1.25 to 1.5 m^3 of brine per ton of injected CO_2, those treatment costs translate to \$0.40 to \$1.20/ton of CO_2. Offsetting that cost would be the market value of produced fresh water. As discussed in Section 3, brine production has the potential of increasing CO_2-well injectivity, which can reduce the total number of required wells and CO_2 compression cost.

The capacity of currently operating RO desalination plants is large compared to the scale of net brine reduction associated with ACRM as discussed in this paper. The Perth, Australia seawater RO desalination plant has been operating since 2006 with a capacity of 52 million m^3 per year (Sanz and Stover, 2007). This plant has an overall recovery rate of 42% and consumes less than 4.2 kWe-h/m^3 of permeate, including intake, pretreatment, both RO passes, post-treatment, potable water pumping, and all electrical losses. Applied to ACRM and an extraction ratio of one, a plant of this scale could consume enough brine to sequester between 35 and 46 million tons of CO_2 per year; which is the amount of CO_2 emitted from coal plants generating 4.4–5.8 GWe. It is worth noting that the desalination capacity of the Perth RO plant is an order of magnitude larger than what would be required for the ACRM cases analyzed in Section 3 of this paper.

There is an expanding industrial experience base in the use of saline cooling water. One sector (Maulbetsch and DiFilippo, 2010) consists of otherwise conventional power plants that use estuarine water or seawater in slightly oversized cooling towers. The second sector (Duke, 2007) consists of power plants that utilize the "zero liquid discharge" (ZLD) concept, in which no residual liquid is returned to the original source. ZLD attempts to vaporize a large fraction of the water in the cooling process by making a large number of cycles so as to minimize the amount of blowdown for final disposal. In ZLD, the input water is usually pretreated by softening, normally by ion exchange. This reduces the scaling potential associated with Ca and Mg. Another pretreatment is to raise the pH, which acts to prevent precipitation of silica. These steps appear to not only effectively control scaling, but also metal corrosion (Duke, 2007).

After treatment to ensure chemical compatibility, brine can be utilized directly as injected make-up water for pressure support of oil and gas production, enhanced geothermal systems, and geothermal power recovered from hydrothermal systems (Harto and Veil, 2011). Enhanced geothermal systems (EGS) are typically located in geologic settings lacking formation water and permeability (MIT, 2006). Hence, EGS may require water to stimulate fracture permeability, act as a working fluid, and to make up for injected water lost to the formation. Primary issues are chemical compatibility with the receiving formation and cost of brine transportation between the CO_2-storage formation and brine-receiving formation (Harto and Veil, 2011). For crude oil production, the rates of co-produced water can be large compared to brine production for ACRM. In the state of Wyoming, 2.12 billion barrels (337 million m^3) of water were co-produced in 2002, along with 54.7 million barrels of oil (Veil et al., 2004). Applied to ACRM, brine production of this scale would sequester between 225 and 270 million tons of CO_2 per year, which is the amount of CO_2 emitted from coal plants generating about 28–34 GWe.

Geothermal energy can be directly recovered from the produced brine to help offset the increased operational cost, when combined with one of the previous volume reduction methods. Geothermal energy production can be limited by pressure depletion, whereas pressure buildup is the limiting consideration for CO_2 storage capacity and security. These two complementary systems can be integrated synergistically, with CO_2 injection providing pressure support to maintain the productivity of geothermal wells, while the production of geothermal brine provides pressure relief and improved injectivity for CO_2-injection wells (Buscheck, 2010;

Author's personal copy

Buscheck et al., 2011b). An integrated geothermal–CCS system, actively managed to yield a volumetric balance between injected and produced fluids, mitigates the risks of reservoir overpressure (CCS concern) or underpressure (geothermal concern), including induced seismicity, insufficient well productivity or injectivity, subsidence, and fluid leakage either to or from overlying formations.

1.4. Objectives of this study

From a reservoir-performance perspective, the key objective for ACRM is for brine production to relieve pressure buildup driven by CO_2 injection. Another perhaps less intuitive objective is to reduce total operating costs of CO_2 storage, on a per unit of stored-CO_2 basis, through the reduction of the total number of wells and the cost of CO_2 compression. Other components of CO_2 storage cost are infrastructure costs, such as those related to obtaining mineral rights, liability insurance, site characterization, and monitoring. As discussed in Section 3, ACRM has the potential of reducing many of these costs. These and other costs, such as those associated with the disposition of the produced brine, are likely to be site specific. Because of the breadth and complexity of determining total CO_2 storage costs, it is beyond the scope of this paper. We defer economic analyses of the net cost (and benefit) of ACRM to future studies.

Brine production can eventually cause CO_2 breakthrough at brine producers. The operational challenge for ACRM is that pressure relief increases with decreasing spacing between CO_2 injectors and brine producers, while CO_2-breakthrough time decreases. Thus, there is a tradeoff between achieving sufficient pressure relief and delaying CO_2 breakthrough. There are several operational strategies that can better achieve this trade-off. One strategy is to successively produce brine from a series of production wells that are incrementally spaced farther from the injection well (Buscheck et al., 2011a,c). A second strategy, which could be used in combination with the first strategy, involves the use of horizontal injection and production wells. A third strategy, which could be combined with the other strategies, is the use of "smart wells" (Brouwer et al., 2001; Brouwer and Jansen, 2004; Sudaryanto and Yortsos, 2001; Alhuthali et al., 2007), with down-hole sensors and multiple independently controlled production and injection zones to extend the useful lifetime of brine-production wells beyond when CO_2 is first detected.

For this study, we conduct reservoir analyses to investigate the first strategy of producing brine from successively increasing distances from the injection well, applied to vertical injectors and producers, and then investigate the second strategy, for horizontal injector/producer-well pairs. We defer the investigating the third strategy (smart wells) to future studies. For the vertical-well study we apply the conceptual model used in earlier studies (Buscheck et al., 2011c; Zhou et al., 2008), which considered homogeneous formations. For the horizontal-well study, we modify that conceptual model to include a wide range of storage-formation thickness, dipping and level formations, various caprock thicknesses, and heterogeneous permeability distributions. We also investigate the sensitivity of pressure relief and CO_2 breakthrough to the key hydrologic parameters.

2. Methodology

In this study, we used the NUFT (Nonisothermal Unsaturated-saturated Flow and Transport) code, which was developed at Lawrence Livermore National Laboratory to simulate multi-phase multi-component heat and mass flow and reactive transport in unsaturated and saturated porous media (Nitao, 1998; Buscheck et al., 2003; Johnson et al., 2004a,b; Carroll et al., 2009; Morris et al., 2011). The pore and fluid compressibility are 4.5×10^{-10} and 3.5×10^{-10} Pa^{-1}, respectively. Water density is determined by the ASME steam tables (ASME, 2006). The two-phase flow of CO_2 and water was simulated with the density of supercritical-CO_2 determined by the correlation of Span and Wagner (1996) and viscosity determined by the correlation of Fenghour et al. (1998). Because we focused on the response in the storage formation and adjoining seal units, the simulations were conducted for isothermal conditions at a fixed temperature of 45 °C. Because we did not consider the reinjection of brine in our study, we did not address salinity-dependent brine density and viscosity. The influence of salinity-dependent brine density and viscosity will be addressed in future work that will consider reinjection of residual brine. Also, the influence of geomechanical coupling (Morris et al., 2011) and geochemical reactions resulting from CO_2 injection were not considered.

Table 1
Summary of hydrologic property values used in the study.

Property	Storage formation	Caprock seal
Horizontal and vertical permeability (m^2)		
Homogeneous case	10^{-13}	10^{-18}
Heterogeneous case 1	10^{-13} and 10^{-14}	10^{-18}
Heterogeneous case 2	10^{-13} and 10^{-15}	10^{-18}
Pore compressibility (Pa^{-1})	4.5×10^{-10}	4.5×10^{-10}
Porosity	0.12	0.12
van Genuchten (1980) m	0.46	0.46
van Genuchten α (Pa^{-1})	5.1×10^{-5}	5.1×10^{-5}
Residual supercritical CO_2 saturation	0.05	0.05
Residual water saturation	0.30	0.30

To simulate CO_2 injection and brine production, we applied two model geometries: (1) 3-D models of a vertical CO_2 injector surrounded by a ring (or rings) of vertical brine producers (Fig. 1a) and (2) 2-D vertical-cross-sectional models of horizontal injector/producer pairs. The numerical grid refinement used in the models is as follows:

- 3-D models of vertical wells: 200-m × 200-m horizontally by 10- to 25-m vertically
- 2-D models of horizontal wells: 200-m horizontally by 20-m vertically

The 3-D models used in the vertical-well study (Section 3.1) represent a 250-m-thick storage formation, as modeled by Zhou et al. (2008) and Buscheck et al. (2011c), with the top of the storage formation located 1200 m below the water table and bounded by 60-m-thick seal units. The outer boundaries have a no-flow condition to represent a semi-closed system for a 1256-km^2 storage formation. The lower boundary of the model, 1800 m below the water table, has a no flow condition. The upper 1140 m and lower 290 m of the model, called the overburden and underburden, have the same hydrologic properties as the CO_2 storage formation. Hydrologic properties of the storage formation and seal units (Table 1) are similar to previous studies (Zhou et al., 2008; Buscheck et al., 2011c), except that a seal permeability of 10^{-18} m^2 is used. CO_2 injection occurs in a 50-m × 50-m zone in the lower half of the storage formation, at a rate of 3.8 million tons/year for an injection period of 30 years, unless otherwise noted. Note that in this study brine production always occurs at a specified rate. Brine is produced in the lower half of the storage formation in 100-m × 100-m zones. For the cases with brine production, we maintained a volumetric balance between produced brine and injected CO_2. We did not explicitly represent reinjection of brine in our study. The vertical-well study only considered homogeneous permeability in the storage formation.

Author's personal copy

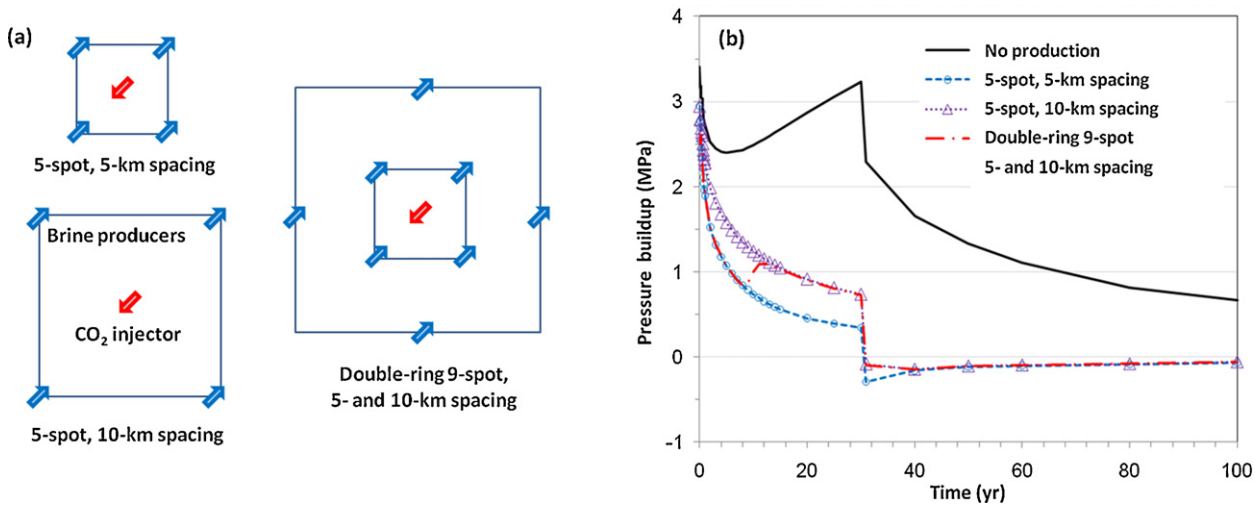

Fig. 1. (a) A plan view of the well patterns analyzed in the vertical-well study, including 5-spot patterns with 5- and 10-km spacing between the CO_2 injector and brine producers and a double-ring 9-spot pattern with 5- and 10-km well spacing. Note that the 5-spot pattern with 3-km well spacing is not shown. (b) Pressure buildup histories in the storage formation adjacent to the top of the CO_2 injector for 5-spot patterns with producers at 5 and 10 km, respectively, and of a double-ring 9-spot pattern (see Fig. 1a), with brine production at the 4 inner producers at 5 km for the first 10 years, ramping from full to zero production from 10 to 15 years. At 10 years, brine production begins at the 4 outer producers at 10 km, ramping from zero to full production from 10 to 15 years, and continuing until the end of injection. CO_2 injection rate is 3.8 million tons/year for 30 years.

The 2-D cross-sectional models used in the horizontal-well study (Section 3.2) included one representing a level storage formation (dip angle of 0°) and the other representing a storage formation with a 10% slope (dip angle of 5.7°), which is in the range of dip angles found in typical sedimentary formations. The models represent a semi-closed reservoir system that is 40 km in the lateral direction (orthogonal to the well axes) and 4 km in the longitudinal direction (parallel to the well axes), with no-flow boundaries at the basement of the storage formation and at the lateral and longitudinal boundaries. This is representative of a semi-closed system for a 160-km^2 storage formation. For level formations, calculations were also made for a 1600- and 16,000-km^2 storage formation to investigate the influence of basin size. Storage-formation thicknesses of 50, 100, 200 and 400 m are considered, underlain by an impermeable basement and overlain by a caprock unit with thicknesses of 50, 100, 200, and 400 m. A constant pressure boundary is maintained at the top of the caprock. For the model with level formations, the basement is 1800 m below the water table. For the model of the dipping formations, the basement is 1800 to 4800 m below the water table. Hydrologic property values (Table 1) are the same as those used in the vertical-well study.

The horizontal-well study also considered cases using a simple conceptual model of layered heterogeneity in the storage formation, with 40-m-thick layers of alternating high and low permeability and permeability contrasts of 10 and 100. The homogeneous and layered-heterogeneous conceptual models used in this study are useful and appropriate for conducting the very broad range of sensitivity analyses addressed in this study. Real sites will have randomly distributed heterogeneity. More realistic representation of heterogeneity, with randomly distributed permeability pertaining to real sites, will be considered in future studies of ACRM. The CO_2 injection well is located at the lowermost 20 m of the storage formation. The brine-production well is also located at the lowermost 20 m of the storage formation, either 5, 10, 15, or 20 km from the injection well. For the dipping case, the brine-production well is located downdip of the CO_2 injection well. Injection periods of 30 to up to 100 years are considered. CO_2 injection rates of 0.475, 0.95, 1.9, 3.8, and 7.6 million tons/year are considered. Because a 2-D model is used, the injection rate is distributed over a longitudinal distance of 4 km.

We conducted grid-sensitivity analyses (Section 3.3) to demonstrate the insensitivity of the reservoir analyses to the numerical grid refinement used in this study. We also conducted a parameter-sensitivity study (Section 3.4) that showed pressure buildup and CO_2 breakthrough time to be most sensitive to storage-formation permeability and insensitive to all other hydrologic parameters except caprock-seal permeability, which only affects pressure buildup for cases with no brine production.

3. Results

The following two sections discuss vertical- and horizontal-well studies of operational strategies to achieving adequate reservoir pressure relief, while delaying CO_2 breakthrough at brine producers. We also investigate how brine production from a horizontal well can manipulate CO_2 migration from a horizontal injector.

3.1. Vertical-well study

We consider CO_2 injection from a single vertical well and analyze the influence of brine production from patterns of vertical wells. We first examine the relationship between pressure relief of pressure buildup at the CO_2 injector and the distance between the CO_2 injector and the brine producers. We then compare two approaches to reservoir-pressure management: with and without brine production.

3.1.1. Relationship between pressure relief and spacing between the CO_2 injector and brine producers

We analyzed three 5-spot patterns, with brine producers at the corners of the patterns, spaced 3, 5 and 10 km from the CO_2 injector at the center of the pattern (Fig. 1a). The case with no brine production was also analyzed. The CO_2 injection rate is 3.8 million tons/year for 30 years and a volumetric balance is maintained between injected CO_2 and produced brine. For these cases, the storage formation has an area of 1256 km^2.

The influence of brine production on pressure relief in the storage formation adjacent to the CO_2 injector decreases with increasing well spacing and increases with time (Table 2). For all cases, pressure buildup (ΔP) immediately builds up to a peak value

Author's personal copy

Table 2
Pressure-buildup in the storage formation adjacent to the top of the CO_2 injector for an injection rate of 3.8 million tons/year for 30 years for 5-spot patterns with well spacings of 3, 5, and 10 km between the CO_2 injector and brine producers.

Time (yr)	Peak pressure buildup (MPa)			
	No brine production	Brine production at the indicated well spacing		
		3 km	5 km	10 km
0.01	2.95	2.95	2.95	2.95
1.0	2.72	1.51	1.90	2.28
5.0	2.40	0.66	1.07	1.58
10.0	2.49	0.41	0.74	1.24
15.0	2.68	0.29	0.56	1.05
20.0	2.87	0.23	0.46	0.92
30.0	3.23	0.14	0.35	0.74
31.0	2.29	−0.34	−0.29	−0.08
100.0	0.66	−0.09	−0.06	−0.06

of 2.95 MPa (Table 2). At 0.01 years it is too early for brine production to influence ΔP for any of the well spacings. The initial decline in ΔP corresponds to the fact the injection well is perforated in the lower half of the storage formation and that it takes time for the influence of the overlying low-permeability caprock to influence pressures adjacent to the CO_2 injector. After the pressure perturbation fully feels the influence of the overlying caprock, ΔP adjacent to the CO_2 injector begins to increase for the no-production case, which continues to increase for the duration of the 30-year injection period. For the cases with brine production, the influence of brine production on relieving ΔP occurs prior to pressure interference with the overlying caprock.

For this discussion we define pressure relief to be the reduction of ΔP with brine production divided by ΔP without brine production. Within 1 year, the CO_2 injector experiences pressure relief for all well spacings. Within 5 years, pressure relief is at least 50% for well spacings of 3 and 5 km; at 10 years, pressure relief is at least 50% for all well spacings. After injection ceases, ΔP around the CO_2 injector abruptly drops to small negative values (slightly below ambient pressure) for all well spacings, while for the no-production case, ΔP persists beyond 100 years. With brine production, buoyancy is the only post-injection driving force for CO_2 and brine migration, which is small (compared to injection-driven ΔP) for CO_2 migration and negligible for brine migration. The large persistent post-injection ΔP for the no-production case will continue to drive CO_2 and brine migration, while for cases with brine production, CO_2 migration will be minor, largely occurring updip, fully within the storage formation, while outward brine migration will virtually cease. When buoyancy is the only driving force, leakage up abandoned wells and faults is less of a concern. The large reduction of post-injection ΔP resulting from brine production could have a positive impact on post-injection monitoring requirements and on the cost of liability insurance.

From the insights gained concerning the relationship between the pressure relief and well spacing, we developed a well pattern, called the double-ring 9-spot (Fig. 1a), which is an example of the pressure-management strategy where brine is produced from multiple rings of brine producers spaced incrementally farther from the CO_2 injector. This pattern has an inner ring of 4 producers 5 km from the CO_2 injector and an outer ring of 4 producers 10 km from the CO_2 injector (Fig. 1a). The outer ring of producers is rotated by 45° relative to the inner ring in order to "pull" on the CO_2 plume from different directions, thereby manipulating the plume into a cylindrical shape. Brine production occurs entirely from the inner 4 producers during the first 10 years; during the next 5 years, brine production is gradually shifted to the outer 4 producers, while maintaining the same total brine production rate.

For the first 10 years, the ΔP history for the double-ring 9-spot follows that of the 5-spot with 5-km spacing (Fig. 1b). As brine production is shifted to the outer ring of producers, the ΔP history for the double-ring 9-spot shifts from that of the 5-spot with 5-km spacing to that of the 5-spot with 10-km spacing. Thereafter, the ΔP history of the double-ring 9-spot follows that of the 5-spot with 10-km spacing.

3.1.2. Comparing pressure management approaches: ACRM versus injection-only

To illustrate two approaches to achieving pressure management, we modified the double-ring 9-spot example, with 60 years of injection. The first (ACRM) approach primarily relies on brine production to achieve a desired ("target") value of ΔP_{peak}. The second (injection-only) approach relies entirely on adjusting the CO_2 injection rate to achieve a target value of ΔP_{peak}. For this example, we chose a ΔP_{peak} target of 1.08 MPa, because it is close to the value of ΔP at 5 years (1.07 MPa) for the case with brine producers at 5 km (Table 2). In general, a target value of ΔP_{peak} would be related to mitigating risks, such as those related to the potential for fracture initiation (Morris et al., 2011) or fault activation (Rutqvist et al., 2007).

The no-production case with a constant CO_2 injection rate of 3.8 million tons/year for 60 years (Fig. 2b) results in an initial ΔP_{peak} of 2.95 MPa and an ultimate ΔP_{peak} of 4.06 MPa, occurring at the end of injection (Fig. 2a). For the double-ring 9-spot case with a constant initial CO_2 injection rate of 3.8 million tons/year, ΔP is initially 2.95 MPa, declining to 1.07 MPa at 5 years. To keep ΔP just at the target value (1.08 MPa), CO_2 injection rate is reduced to an initial value of 1.2 million tons/year, ramped up to 4.0 million tons/year at 5 years, and held constant until 15 years (Fig. 2b). The yellow area in Fig. 2a represents the "overpressure", relative to the ΔP target, while the yellow area in Fig. 2b represents the required reduction in CO_2 injection rate to stay within the ΔP target. At 15 years, brine production has completely shifted to the outer 4 producers at 10 km. Brine production at 10 km results in a ΔP of 1.05 MPa at 15 years (Table 2), which is just below the target value. Because pressure relief from brine production at 10 km increases with time, it is possible to continuously ramp up the CO_2 injection rate from 4.0 to 8.6 million tons/year for duration of the injection period (Fig. 2b) and remain close to the ΔP target (Fig. 2a). To keep ΔP at the target value for the no-production case, CO_2 injection rate is reduced to an initial value of 1.1 million tons/year, slowly increased to 1.5 million tons/year at 5 years, then gradually reduced to 0.7 million tons/year at 60 years.

A way to quantify the pressure-relieving benefit of brine production is the injectivity ratio, determined by dividing CO_2 injection rate for the ACRM case by CO_2 injection rate for the no-production case for the same value of ΔP. Thus, injectivity ratio varies continuously with time. For this pressure-management example, the injectivity ratio starts at a value of 1.1, increasing to 2.7, 5.4, and 12.2 at 5, 30, and 60 years, respectively. For the 60-year injection period, brine production enables a 5.5-fold increase in stored CO_2, compared to the no-production case.

3.2. Horizontal-well study

We consider CO_2 injection from a single horizontal well and analyze the influence of brine production from a single horizontal well at distances of 5, 10, 15, and 20 km from the CO_2 injector. We investigate the influence of brine production on CO_2 plume migration, pressure buildup (ΔP) in the storage formation adjacent to the CO_2 injector, injectivity of the CO_2 injector, and CO_2 breakthrough at the brine producer.

Author's personal copy

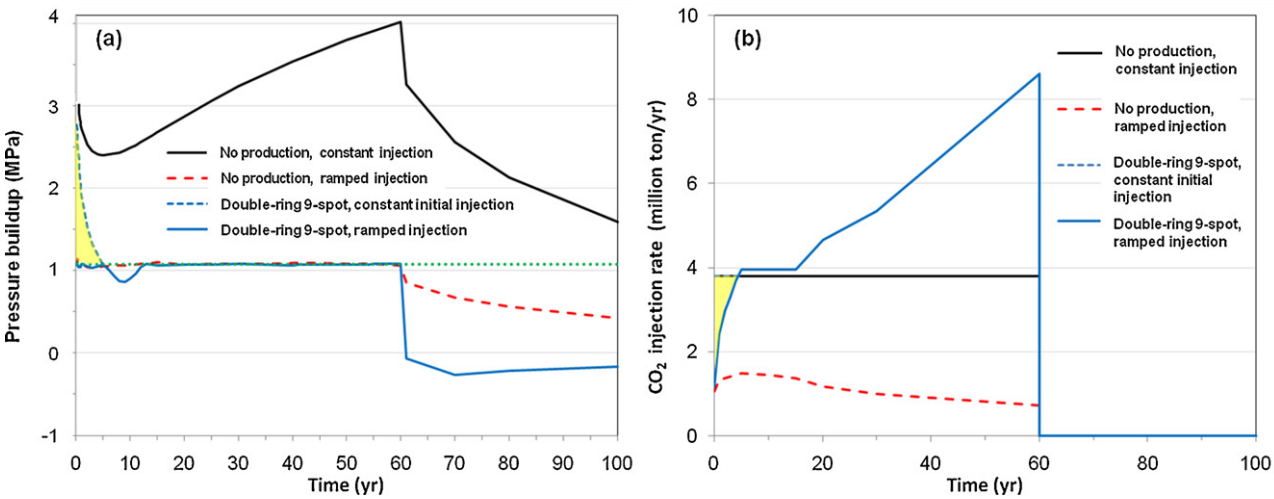

Fig. 2. Pressure buildup history in the storage formation adjacent to the top of the CO_2 injector (a) and CO_2 injection rate (b) are plotted for two "no-production" cases and two "double-ring 9-spot" cases, all with 60 years of injection. The no-production cases include "constant injection" with a CO_2 injection rate of 3.8 million tons/year and "ramped injection" with injection rate reduced just enough to keep pressure buildup below a specified value (dotted green curve). The double-ring 9-spot cases only differ by virtue of the initial CO_2 injection rates, as depicted by the yellow area in (b), with "constant initial injection" having an initial rate of 3.8 million tons/year and "ramped injection" having the initial rate reduced just enough to keep pressure buildup below the "target" value. The yellow area in (a) shows the influence that the initial CO_2 injection rate reduction has on pressure buildup. Later, the CO_2 injection rate for the double-ring 9-spot cases is gradually increased just enough to keep pressure buildup below the target value.

3.2.1. *Manipulating CO_2 plume migration*

The use of brine production to manipulate/steer the CO_2 plume has been analyzed for CO_2 injection from a single vertical well surrounded by rings of vertical production wells (Buscheck et al., 2011c; Court, 2011). Figs. 3 and 4 from Buscheck et al. (2011c) showed significant steering potential; however, those analyses are applicable to many rings of CO_2 brine producers, which is unlikely to be economically practical. Court (2011) found a single ring of 4 vertical production wells, placed outside of the outer extent of the CO_2 plume (in order to avoid CO_2 breakthrough), has negligible steering potential on the CO_2 plume and they concluded that more complex vertical-well strategies would need to be investigated. In this section, we investigate the effectiveness of CO_2-plume manipulation/steering for a horizontal injector/producer-well pair.

We examine the influence of brine production on CO_2 plume migration in dipping storage formations, for cases with homogeneous and heterogeneous permeability in the storage formation. We consider a CO_2-storage formation that is 400 m thick, overlain by a 400-m-thick caprock, and with a 10% slope (5.7° dip angle). The brine producer is located 10 km downdip from the CO_2 injector and the injection period varies, depending on when CO_2 breakthrough occurs. Supercritical CO_2 largely flows preferentially through the high-permeability layers (Fig. 3), while diffusion of aqueous-phase CO_2 distributes CO_2 into the low-permeability layers (Fig. 4).

Homogeneous permeability in the storage formation allows buoyancy to strongly drive CO_2 updip for the case with no brine production (Figs. 3a and 4a). The addition of brine production 10 km downdip of the CO_2 injector largely negates the influence of buoyancy (Figs. 3b and 4b), pulling the CO_2 plume down to the brine producer, where breakthrough occurs at 46 years. The influence of layered heterogeneous permeability in the storage formation impedes the buoyancy-driven migration of the CO_2 plume (Figs. 3c and 4c). When the permeability contrast is increased, layered heterogeneity more strongly impedes the buoyancy-driven migration of the CO_2 plume (Figs. 3e and 4e), so much so that the CO_2 plume is almost symmetrical about the CO_2 injector. For the ACRM case, layered heterogeneous permeability in the storage formation causes the CO_2 plume to be more evenly distributed vertically in the storage formation, which delays the arrival of the CO_2 plume at the brine producer, increasing breakthrough time to 50 years (Figs. 3d and 4d). When the permeability contrast is increased, layered heterogeneity much more evenly distributes the CO_2 plume vertically in the storage formation, which further delays the arrival of the CO_2 plume at the brine producer, increasing breakthrough time to 75 years (Figs. 3f and 4f).

3.2.2. *Pressure relief and injectivity*

We consider the relationship between ΔP_{peak}, injectivity, and CO_2 breakthrough time, starting with a 400-m-thick storage formation with an area of 160 km^2. ΔP_{peak} increases with CO_2 injection rate and well spacing between the producer/injector pair (Fig. 5a and Table 3). The pressure-relieving effect of brine production is seen as a reduction in slope of ΔP_{peak} versus CO_2 injection rate (Q_{inj}) curve. Because pressure relief increases with decreasing well spacing, the slope is reduced with decreasing well spacing. Conversely, with increasing well spacing, the ΔP_{peak} versus Q_{inj} slope increases; for large enough well spacing, it approaches that of the no-production case.

Heterogeneity has a modest influence on ΔP_{peak} for the no-production case, while for cases with brine production the influence on ΔP_{peak} is much stronger. Compared to the homogeneous case, the heterogeneous case has the effective permeability in the horizontal direction reduced by 45% (5.5×10^{-14} m^2 versus 1.0×10^{-13} m^2). Accordingly, the influence is equivalent to nearly doubling the well spacing for a level formation (Table 3).

As discussed earlier, injectivity ratio is a useful way to quantify the pressure-relieving benefit of brine production. For the horizontal-well study, we define the injectivity ratio with respect to the ΔP_{peak}, rather than for the ΔP at a specific point in time. Thus, injectivity ratio is the CO_2 injection rate for the ACRM case divided by the CO_2 injection rate for the no-production case for the same value of ΔP_{peak}. For the horizontal-well study, injectivity ratio pertains to the injection period as a whole. Because the ACRM case has twice the number of wells as the no-production case and because the CO_2 injector and brine producer have the same perforated lengths (4 km), an injectivity ratio greater than 2 indicates a savings in well-drilling costs. Thus, improved injectivity facilitated by ACRM may reduce well-drilling costs. In the following analyses brine production in horizontal wells was always found to result in

Author's personal copy

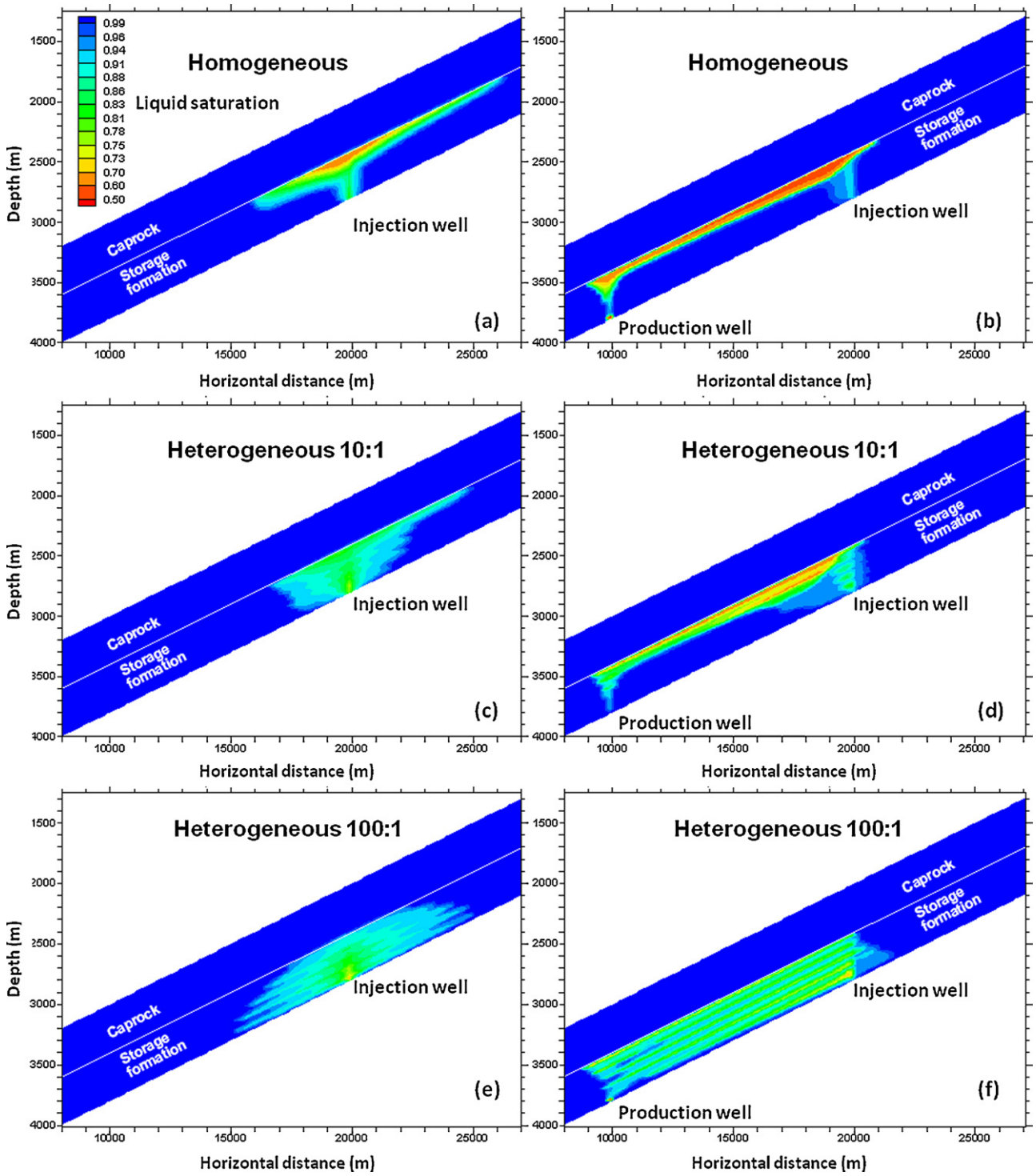

Fig. 3. Liquid saturation contours show CO_2-plume migration driven by CO_2 injection from a horizontal well for no brine production (a, c, and e), and for brine produced in a horizontal well 10 km downdip from the injection well (b, d, and f). Storage-formation-permeability cases are (1) homogeneous (a and b), (2) layered heterogeneity with a permeability contrast of 10 (c and d), and (3) layered heterogeneity with permeability contrast of 100 (e and f). The heterogeneous cases have alternating 40-m-thick layers of high and low permeability. The horizontal injectors and producers are located in the lower 20 m of the storage formation. The formation dip angle is 5.7° and the vertical scale in the plot is exaggerated by a factor of 5.

an injectivity ratio greater than 2, with injectivity ratio often being much greater than 2.

Because pressure relief decreases with increasing well spacing, injectivity ratio also decreases with well spacing (Fig. 5b). Injectivity ratio is seen to be relatively insensitive to CO_2 injection rate, as evidenced by similar injectivity ratio versus well spacing curves for CO_2 injection rates of 3.8 and 7.6 million/year. Because ΔP_{peak} is more sensitive to heterogeneity for the ACRM cases than for the no-production cases, injectivity ratio is less in the heterogeneous cases. It is worth noting that if the average horizontal permeability been kept fixed between the homogeneous and heterogeneous cases, it is likely that the injectivity ratio would not have been reduced by us much as a factor of 2 in the heterogeneous case. Therefore, what is actually being exhibited is that injectivity ratio decreases with

Author's personal copy

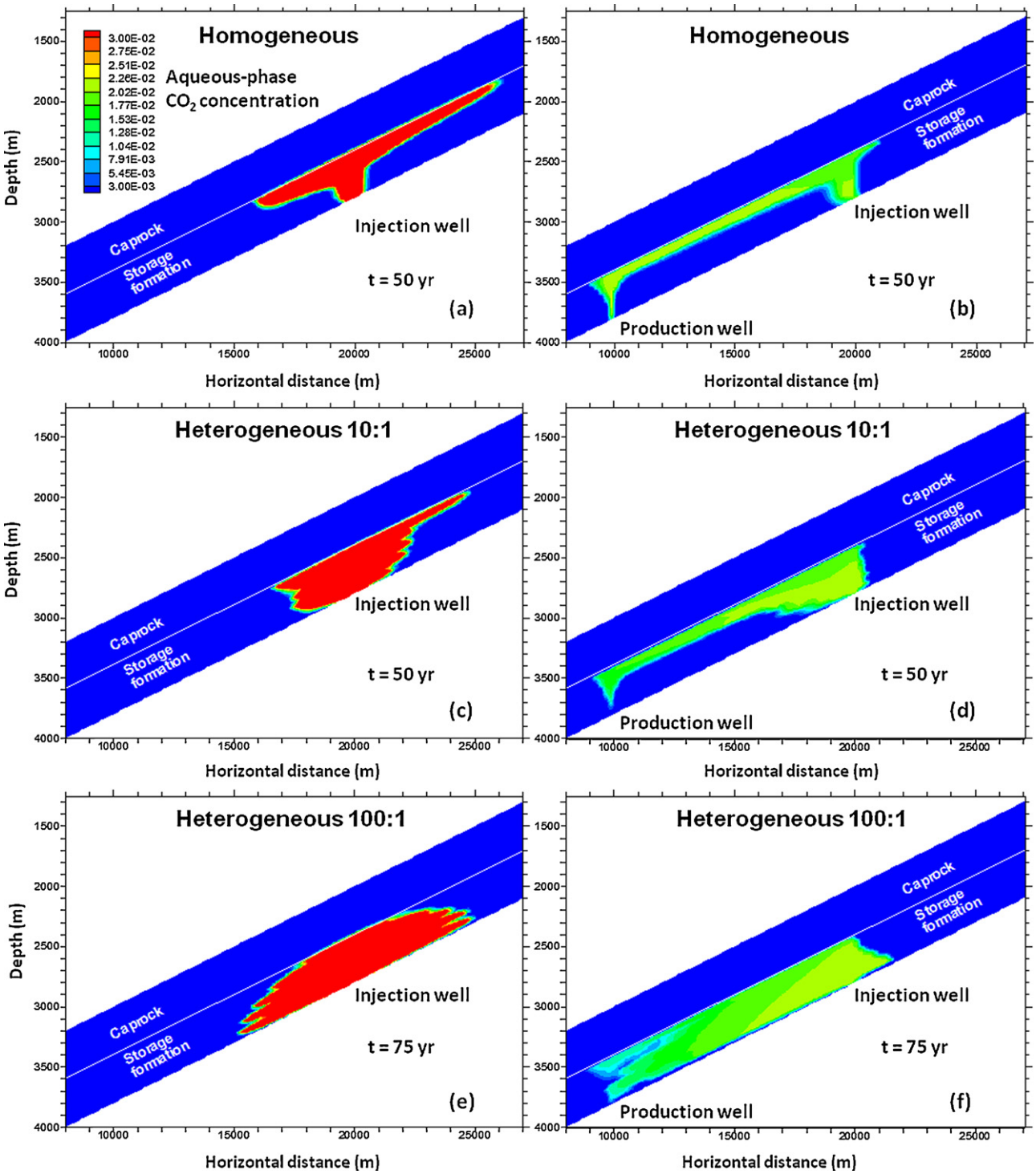

Fig. 4. Aqueous-phase CO_2-concentration contours show CO_2-plume migration driven by CO_2 injection from a horizontal well for no brine production (a, c, and e), and for brine produced in a horizontal well 10 km downdip from the injection well (b, d, and f). Storage-formation-permeability cases are (1) homogeneous (a and b), (2) layered heterogeneity with a permeability contrast of 10 (c and d), and (3) layered heterogeneity with permeability contrast of 100 (e and f). The heterogeneous cases have alternating 40-m-thick layers of high and low permeability. The horizontal injectors and producers are located in the lower 20 m of the storage formation. The formation dip angle is 5.7° and the vertical scale in the plot is exaggerated by a factor of 5.

decreasing permeability, not necessarily by virtue of the existence of heterogeneity.

3.2.3. CO_2 breakthrough at brine producers

As expected, CO_2 breakthrough time increases with well spacing (Fig. 6a). Because of the large thickness of the storage formation (400 m) and the CO_2 injector and brine producer being at the bottom of the storage formation, the slope of the CO_2 breakthrough time versus well spacing curve is less than 1 for smaller well spacing, increasing to a slope of nearly 1 for larger well spacing. The CO_2 plume rises to, and flows along, the top of the storage formation, until it overlies the brine producer, where it is pulled downward to the brine producer. For smaller well spacing, the vertical travel distance is a significant portion of the overall travel distance between

Author's personal copy

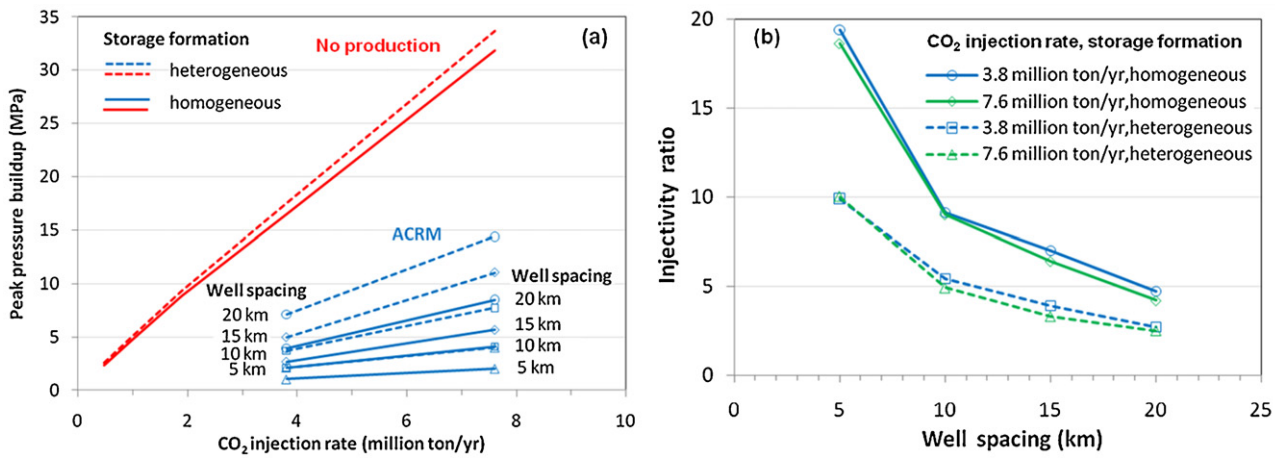

Fig. 5. (a) Peak pressure buildup in the storage formation adjacent to the CO_2 injector versus CO_2 injection rate is plotted for horizontal-well cases with no brine production and with brine produced from producers spaced 5, 10, 15, and 20 km from the injector. The storage formation is level, 400 m thick, overlain by a 400-m thick caprock. Heterogeneous cases have alternating 40-m-thick layers of high and low permeability, with a permeability contrast of 10. (b) Injectivity ratio is plotted versus well spacing between injector/producer pairs for CO_2-injection rates of 3.8 and 7.6 million tons/year. The injection period is 30 years and storage-formation area is 160 km^2.

Table 3
Pressure buildup in the storage formation adjacent to the CO_2 injector is listed for cases with no brine production and with brine production wells at the indicated spacing for a 400-m-thick storage-formation with an area of 160 km^2. CO_2 injection rate of 3.8 million tons/year. For the cases with brine production, peak pressure buildup occurs at the beginning of the injection period.

Storage-formation permeability distribution	Formation dip angle (degrees)	No brine production pressure buildup (MPa) at indicated time				Brine production at the indicated well spacing peak pressure buildup (MPa)			
		30 yr	50 yr	75 yr	100 yr	5 km	10 km	15 km	20 km
Homogeneous	0	16.8	25.1	34.5	43.2	1.0	2.1	2.7	3.9
	5.7	16.6	24.8	34.7	44.0	0.9	1.9	2.5	3.5
Layered heterogeneous with 10:1 contrast	0	17.5	25.6	35.1	43.9	2.1	3.7	5.0	7.1
	5.7	19.9	27.8	37.5	46.9	2.6	4.9	6.4	8.9
Layered heterogeneous with 100:1 contrast	0	18.8	27.0	36.6	45.5	3.4	4.6	6.0	9.7
	5.7	21.8	29.8	39.2	47.9	4.2	6.8	8.9	11.9

the CO_2 injector and brine producer. For larger well spacing, the vertical distance is a smaller portion of the overall distance. To first order, the CO_2 travel distance is 5.8, 10.8, 15.8, and 20.8 km for the 5-, 10-, 15-, and 20-km well spacings, respectively.

For a level formation, heterogeneity causes preferential flow of CO_2 that reduces CO_2 breakthrough time. For 10-km well spacing and a CO_2 injection rate of 3.8 million tons/year, CO_2 breakthrough occurs at 45 and 30 years for the homogeneous and heterogeneous cases, respectively, while for an injection rate of 7.6 million tons/year, CO_2 breakthrough occurs at 19 and 18 years.

Heterogeneity can have the opposite influence on CO_2 breakthrough time, depending on formation dip and where the brine producer is located, relative to the CO_2 injector. Compared to level placement in a level storage formation, placing a brine producer downdip of the CO_2 injector can increase CO_2 breakthrough time, particularly for heterogeneous storage-formation permeability (Fig. 6b). Therefore, it is possible to take advantage of the

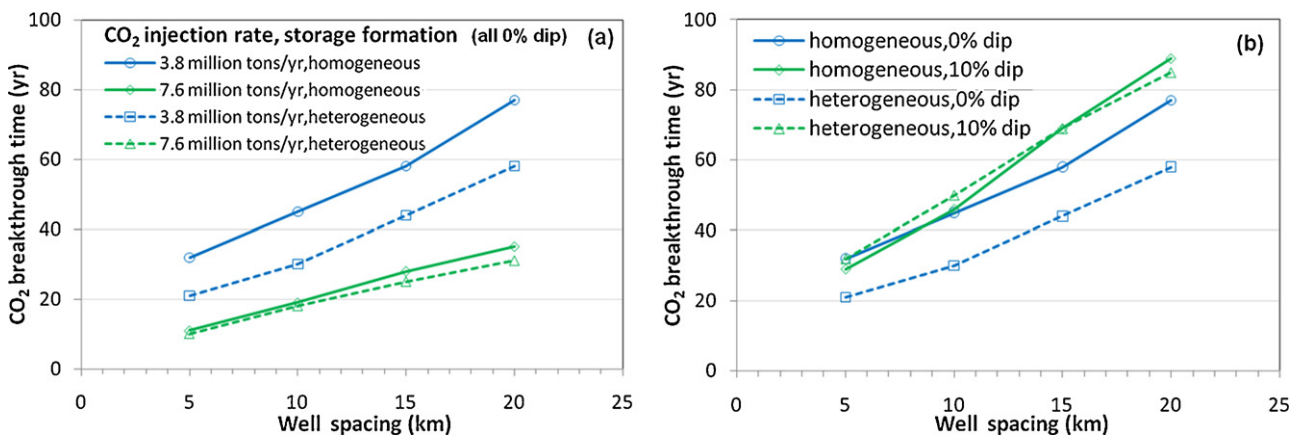

Fig. 6. (a) CO_2 breakthrough time is plotted versus well spacing between horizontal CO_2 injectors and brine producers for the set of ACRM cases plotted in Fig. 5b. (b) The influence of formation dip on CO_2 breakthrough time is shown for a CO_2-injection rate of 3.8 million tons/year. Heterogeneous cases have alternating 40-m-thick layers of high and low permeability, with a permeability contrast of 10. The storage formation is 400 m thick with an area of 160 km^2 and is overlain by a 400-m-thick caprock.

Author's personal copy

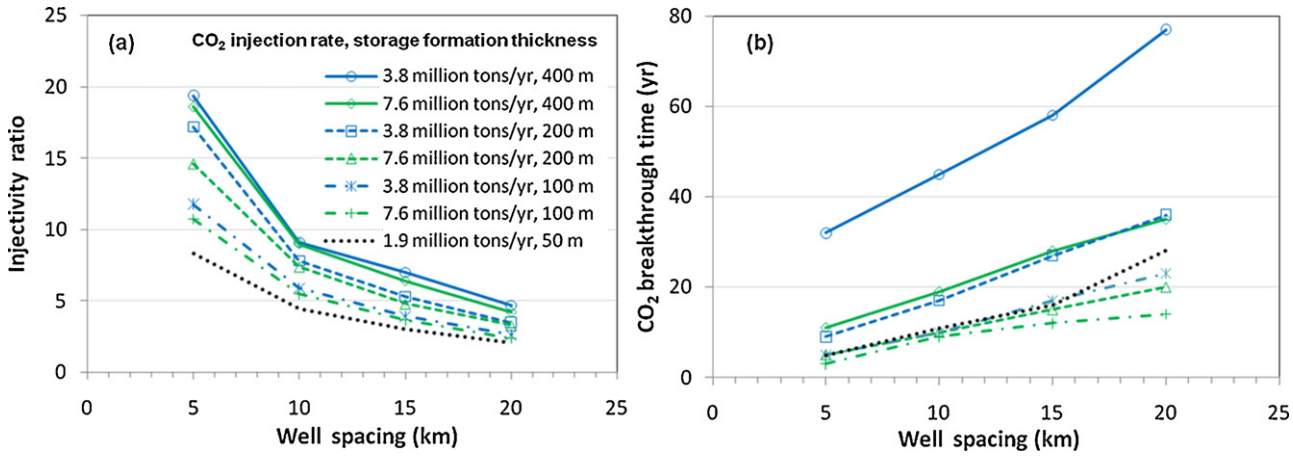

Fig. 7. (a) Injectivity ratio and (b) CO_2 breakthrough time are plotted versus well spacing between horizontal injector/producer pairs for storage-formation thicknesses of 50, 100, 200 and 400 m. The storage formation has homogeneous permeability, the caprock is 400 m thick, the injection period is 30 years, and storage-formation area is 160 km^2.

influence of buoyancy flow with respect to CO_2 breakthrough. The beneficial influence of buoyancy on delaying CO_2 breakthrough increases with dip angle and with permeability contrast (compare Fig. 3d and f).

3.2.4. Influence of storage-formation thickness and area

The previous discussion pertains to a relatively thick (400 m) storage formation and a relatively small storage-formation area (160 km^2). Therefore, we investigated the influence of storage-formation thickness and area on ΔP_{peak} and injectivity, including storage-formation thicknesses of 50, 100, 200 and 400 m and storage-formation areas of 160, 1600, and 16,000 km^2. Injectivity ratio decreases with decreasing storage-formation thickness (Fig. 7a). Reducing storage-formation thickness from 400 to 200 m has a relatively small effect on injectivity ratio. CO_2 breakthrough time is reduced nearly linearly with storage-formation thickness for larger thicknesses (Fig. 7b). For thinner storage formations, the decrease in CO_2 breakthrough time is slightly less than linear because the CO_2 plume occupies a greater portion of the storage formation for thin formations than for thick formations.

We decided to increase the storage formation area by factors of 10 and 100 to see when the influence of increased area has a diminishing effect on pressure buildup and injectivity ratio. In other words, we wanted to establish when the formation was effectively infinite in areal extent. We found that factors of 10 and 100 yielded the same ΔP_{peak} for the no-production case (Fig. 8a); thus, a storage-formation area of 1600 km^2 is effectively infinite in areal extent for this problem. We also found that increasing the storage-formation area by a factor of either 10 or 100 reduces ΔP_{peak} around the CO_2 injector by 30–40% (with this effect increasing with CO_2 injection rate) for the no-production case (Fig. 8a). This is expected because there is considerably greater area for pressure buildup to be dissipated through the caprock and greater storage-formation volume over which fluid compression can occur. For ACRM cases, ΔP_{peak} is insensitive to storage-formation area for well spacings of 5, 10, and 15 km and slightly sensitive for 20-km well spacing (Fig. 8a). Accordingly, increasing the storage-formation area by a factor of 10 has the effect of reducing injectivity ratio by about 30–40% (with this effect increasing with CO_2 injection rate) (Fig. 8b). Injectivity ratios are still much greater than 2 for well spacings of 10 km or less and are greater than 2 for well spacings of 15 and 20 km. Because storage-formation area does not influence CO_2 breakthrough time, it was not necessary to include plots of that influence.

3.2.5. Scalability of CO_2 storage with ACRM

As discussed earlier, the definition of injectivity ratio used in the horizontal-well study is based on ΔP_{peak}, rather than ΔP as a function of time. Because of when ΔP_{peak} occurs for cases with and without brine production, this definition does not fully quantify the beneficial influence of brine production on pressure relief. ΔP_{peak} occurs relatively early during the injection period for cases with brine production (Fig. 9). Without brine production, ΔP increases throughout the injection period, reaching its peak at the end of injection (Fig. 9); ΔP increases nearly linearly with time for a relatively small storage-formation area (Fig. 9a), while the rate of increase of ΔP decreases with time for a storage formation of very large (effectively infinite) areal extent (Fig. 9b).

After ΔP_{peak} occurs, the influence of brine production on pressure relief continues to increase with time. For the 160-km^2 storage formation, this reduces ΔP to zero at 7, 10, and 25 years for well spacings of 5, 10, and 15 km, respectively (Fig. 9a). For the 1600-km^2 case, ΔP is reduced to zero at 8 and 28 years for well spacings of 5 and 10 km, respectively (Fig. 9b). The difference between the small and large storage formation indicates the influence of pressure relief being stronger in a more areally confined storage formation. Because ΔP_{peak} occurs relatively early during injection, ΔP_{peak} is insensitive to storage-formation area. The strong influence of brine production on pressure relief indicates that, after ΔP_{peak} is attained, it should be possible to continuously ramp up the CO_2 injection rate while remaining just below a target value of ΔP, as done in the double-ring 9-spot pressure-management example discussed earlier (Fig. 2). This demonstrates the inherent *scalability* of ACRM and has useful implications on the feasibility of large-scale implementation of CCS. Within a region, as more CCS emitters become equipped to capture CO_2, it would be possible to add their CO_2 output to an existing CO_2-storage operation that utilized ACRM.

We also considered caprock thicknesses of 50, 100, and 200 m, in addition to the cases discussed above that had a 400-m-thick caprock. For this range of caprock thickness, we found that ΔP_{peak}, injectivity ratio, and CO_2 breakthrough time are insensitive to caprock thickness. Thus, it is unnecessary to include any plots of that influence.

3.2.6. Impact of multiple horizontal brine production wells

In this study we limited ourselves a single horizontal brine production well. Consideration of Figs. 5 and 7a, Figs. 8 and 9 indicate the advantage of successively producing brine from more than one horizontal well. For a 400-m-thick formation and an injection rate

Author's personal copy

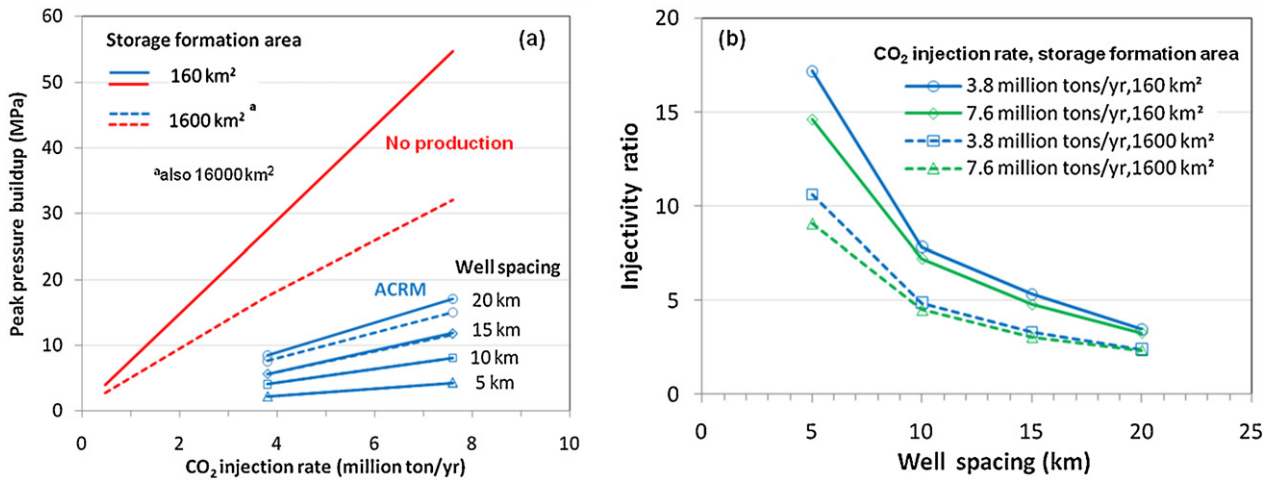

Fig. 8. (a) Peak pressure buildup in the storage formation adjacent to the CO_2 injector versus CO_2 injection rate is plotted for horizontal-well cases with no brine production and with brine produced from horizontal wells spaced 5, 10, 15, and 20 km from the injector for storage-formation areas of 160, 1600, and 16,000 km^2. The storage formation is level, 200 m thick, with homogeneous permeability, and overlain by a 400-m thick caprock. (b) Injectivity ratio is plotted versus well spacing between injector/producer pairs for CO_2-injection rates of 3.8 and 7.6 million tons/year. The injection period is 30 years. Curves for storage-formation areas of 1600 and 16,000 km^2 are the same.

of 3.8 million tons/year, brine production from a well 5 km from the CO_2 injector could increase injectivity by a factor of at least 10 (Fig. 5b). As CO_2 approached the brine producer, at some time greater than 20 years (Fig. 6b), brine production could be gradually shifted to a well 20 km from the CO_2 injector, providing the same degree of pressure relief achieved at early time from the producer at 5 km (Fig. 9), while delaying CO_2 breakthrough to 60 years or more (Fig. 6b). By using two or more horizontal brine producers it could be feasible to sustain an injectivity ratio of 10 or more, and a tenfold increase or greater in storage capacity. The same principal could be also applied to thinner storage formations.

3.3. Grid-sensitivity study

Grid-sensitivity analyses were conducted for the horizontal-well cases for a 400-m-thick storage formation with zero dip. Compared to the *base* mesh used in this study, the vertical and horizontal grid refinement was both decreased and increased by a factor of two, with grid spacing of 400-m horizontally by 40-m vertically for the coarse mesh and 100-m horizontally by 10-m vertically for the fine mesh, versus 200-m by 20-m for the base mesh. Grid refinement has a negligible influence on pressure buildup and CO_2 breakthrough time (Table 4) for the homogeneous case and 10:1 heterogeneous case, demonstrating the insensitivity of our simulations to the numerical refinement used in this study. For the 100:1 heterogeneous case, which was only considered in the dipping formations, the coarse mesh yields a greater CO_2 breakthrough time, while the base and fine meshes produced similar CO_2 breakthrough times.

3.4. Parameter-sensitivity study

Sensitivity analyses of key hydrologic parameters were conducted for horizontal-well cases for a 400-m-thick storage formation with zero dip (Table 3). We start with parameters having a negligible influence on pressure buildup (ΔP) and CO_2

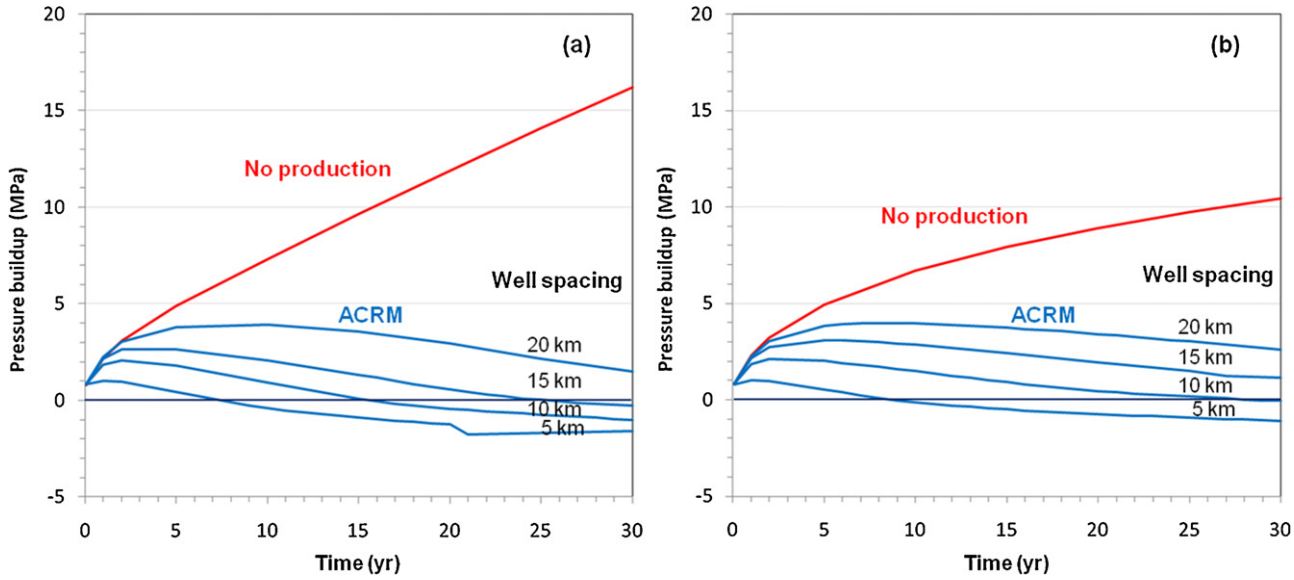

Fig. 9. Pressure buildup history in the storage formation adjacent to the CO_2 injector is plotted for horizontal-well cases with no brine production and with brine produced from horizontal wells spaced 5, 10, 15, and 20 km from the CO_2 injector for a storage-formation area of (a) 160 km^2 and (b) 1600 km^2. The storage formation is level 400 m thick, with homogeneous permeability, overlain by a 400-m-thick caprock. The injection period is 30 years.

Author's personal copy

Table 4
CO_2 breakthrough time and pressure buildup in the storage formation adjacent to the horizontal CO_2 injector are listed for the coarse, standard, and fine numerical mesh for the base case with a 400-m-thick storage formation with an area of 160 km^2 and 400-m-thick caprock.

Dependent variable	Well spacing (km)	Homogeneous			10:1 Heterogeneous			100:1 Heterogeneous		
		Coarse mesh	Base mesh	Fine mesh	Coarse mesh	Base mesh	Fine mesh	Coarse mesh	Base mesh	Fine mesh
CO_2 breakthrough time (yr)	10	45	45	46	32	30	30	52	42	38
	No production	NA	NA	NA	NA	NA	NA	NA	NA	NA
Peak pressure buildup (MPa)	10	2.05	2.08	2.09	3.70	3.69	3.63	4.25	4.61	4.62
	No production	16.75	16.81	16.73	17.70	17.53	17.41	18.87	18.81	18.92

Table 5
CO_2 breakthrough time and pressure buildup in the storage formation adjacent to the horizontal CO_2 injector are listed for a range of storage-formation van Genuchten α. The storage formation is 400-m thick, with an area of 160 km^2, overlain by a 400-m-thick caprock. The base case is shown in bold.

Dependent variable	Well spacing (km)	van Genuchten α (Pa^{-1})				
		5.1×10^{-6}	2.55×10^{-5}	$\mathbf{5.1 \times 10^{-5}}$	1.2×10^{-4}	5.1×10^{-4}
CO_2 breakthrough time (yr)	10	43	45	**45**	45	45
	No production	NA	NA	**NA**	NA	NA
Peak pressure buildup (MPa)	10	2.13	2.09	**2.08**	2.08	2.07
	No production	16.97	16.84	**16.81**	16.79	16.78

Table 6
CO_2 breakthrough time and pressure buildup in the storage formation adjacent to the horizontal CO_2 injector are listed for a range of caprock-seal van Genuchten α. The storage formation is 400-m thick, with an area of 160 km^2, overlain by a 400-m-thick caprock. The base case is shown in bold.

Dependent variable	Well spacing (km)	van Genuchten α (Pa^{-1})		
		5.1×10^{-6}	$\mathbf{5.1 \times 10^{-5}}$	5.1×10^{-4}
CO_2 breakthrough time (yr)	10	45	**45**	45
	No production	NA	**NA**	NA
Peak pressure buildup (MPa)	10	2.08	**2.08**	2.08
	No production	16.81	**16.81**	16.81

Table 7
CO_2 breakthrough time and pressure buildup in the storage formation adjacent to the horizontal CO_2 injector are listed for a range of residual supercritical CO_2 saturation. The storage formation is 400-m thick, with an area of 160 km^2, overlain by a 400-m-thick caprock. The base-case is shown in bold.

Dependent variable	Well spacing (km)	Residual supercritical CO_2 saturation				
		0.05	0.12	0.15	0.25	0.30
CO_2 breakthrough time (yr)	10	**45**	50	53	69	81
	No production	**NA**	NA	NA	NA	NA
Peak pressure buildup (MPa)	10	**2.08**	2.14	2.17	2.25	2.34
	No production	**16.81**	16.99	17.08	17.43	17.66

Table 8
CO_2 breakthrough time and pressure buildup in the storage formation adjacent to the horizontal CO_2 injector are listed for a range of storage-formation porosity. The storage formation is 400-m thick, with an area of 160 km^2, overlain by a 400-m-thick caprock. The base-case is shown in bold.

Dependent variable	Well spacing (km)	Storage-formation porosity		
		0.06	**0.12**	0.24
CO_2 breakthrough time (yr)	10	45	**45**	45
	No production	NA	**NA**	NA
Peak pressure buildup (MPa)	10	2.08	**2.08**	2.08
	No production	16.81	**16.81**	16.81

Table 9
CO_2 breakthrough time and pressure buildup in the storage formation adjacent to the horizontal CO_2 injector are listed for a range of storage-formation permeability. The storage formation is 400-m thick, with an area of 160 km^2, overlain by a 400-m-thick caprock. The base case is shown in bold.

Dependent variable	Well spacing (km)	Storage-formation permeability (m^2)				
		1.0×10^{-14}	5.0×10^{-14}	$\mathbf{1.0 \times 10^{-13}}$	2.0×10^{-13}	1.0×10^{-12}
CO_2 breakthrough time (yr)	5	32	30	**32**	55	246
	10	67	40	**45**	71	250
	No production	NA	NA	**NA**	NA	NA
Peak pressure buildup (MPa)	5	10.20	2.09	**1.03**	0.49	0.11
	10	20.40	4.03	**2.08**	1.02	0.19
	No production	31.61	18.11	**16.82**	16.21	15.73

Author's personal copy

Table 10
CO_2 breakthrough time and pressure buildup in the storage formation adjacent to the horizontal CO_2 injector are listed for a range of caprock-seal permeability. The storage formation is 400-m thick, with an area of 160 km^2, overlain by a 400-m-thick caprock. The base case is shown in bold.

Dependent variable	Well spacing (km)	Caprock-seal permeability (m^2)				
		1.0×10^{-20}	1.0×10^{-19}	$\mathbf{1.0 \times 10^{-18}}$	1.0×10^{-17}	1.0×10^{-16}
CO_2 breakthrough time (yr)	10	45	45	**45**	46	50
	No production	NA	NA	**NA**	NA	NA
Peak pressure buildup (MPa)	10	2.11	2.11	**2.08**	2.06	1.93
	No production	19.57	18.80	**16.82**	12.42	4.16

breakthrough time. Tables 5 and 6 show the negligible influence of van Genuchten α (van Genuchten, 1980), which is inversely proportional to air-entry pressure and a direct measure of capillarity. Table 7 indicates that residual supercritical CO_2 saturation in the storage formation has a negligible influence on pressure buildup and that the value used in this study (0.05) conservatively predicts CO_2 breakthrough time. Table 8 indicates the negligible influence of storage-formation porosity. The most sensitive parameters are storage-formation permeability, followed by caprock-seal permeability. With no brine production, ΔP increases with decreasing $\log_{10}$ of storage-formation permeability, while it increases linearly with decreasing storage-formation permeability for cases with brine production (Table 9). The influence of storage-permeability permeability on CO_2 breakthrough time is related to its influence on buoyancy. The base-case value of storage-formation permeability used in study is close to the value resulting in a minimum CO_2 breakthrough time and is therefore conservative in that sense. Caprock-seal permeability has a negligible influence on ΔP and CO_2 breakthrough time for cases with brine production (Table 10). With the exception of very high permeability values, the influence of caprock-seal permeability on ΔP is roughly half that of storage-formation permeability for cases with no brine production (Tables 9 and 10). Without brine production, brine leakage into the caprock can provide significant pressure relief, while for cases with brine production, the lack of sensitivity to caprock-seal permeability is indicative of minimal brine leakage (Table 10).

4. Summary and conclusions

For injection-only, industrial-scale, saline-formation geologic CO_2 storage, pressure buildup can limit CO_2 storage capacity and security. Moreover, water demand and parasitic energy costs associated with CO_2 capture and storage operations are large. Active CO_2 Reservoir Management (ACRM), which combines brine production with CO_2 injection, has the potential of addressing these challenges. We demonstrate how ACRM can potentially enhance reservoir performance in two important ways. First, it can provide more secure CO_2 storage by enabling pressure relief, spatial and temporal control of brine migration, and CO_2 plume manipulation. Second, it can result in more cost-effective CO_2 storage by improving CO_2 injectivity and storage capacity. Brine production may also enable development of utilization options, including freshwater production, saline cooling water for power plants, geothermal power, and make-up water for oil, gas, and geothermal energy production. These options are important to the economic feasibility of ACRM because they can reduce the volume of brine requiring reinjection.

The key reservoir-performance objective for ACRM is to relieve pressure buildup driven by CO_2 injection. For economic and operational reasons, it is important to delay CO_2 breakthrough at brine producers. We investigated two operational strategies for balancing these objectives: (1) vertical wells with multiple rings of brine producers and (2) horizontal injector/producer-well pairs.

For vertical wells, an injection-only strategy was compared to a pressure-management strategy with brine production from a double-ring 9-spot pattern. Except for early time, pressure management can be entirely achieved with brine production. Because pressure relief increases with time, the CO_2 injection rate can be ramped up, while staying within a pressure-buildup target, while for the no-production case, injection rates must be gradually decreased to stay within target. Brine production causes pressure buildup to abruptly drop to zero after injection ceases, while, without brine production, pressure buildup can persist long after injection ceases.

For horizontal wells, we find that layered heterogeneous permeability in the storage formation causes preferential flow of CO_2, which can reduce CO_2 breakthrough time at brine producers. Brine produced downdip of CO_2 injection can strongly influence CO_2 migration. Without brine production, buoyancy drives CO_2 updip, unless impeded by layered heterogeneity. With brine production, the combination of buoyancy and layered heterogeneity can cause CO_2 to be more evenly distributed vertically in the storage formation, which delays CO_2 breakthrough at the brine producer. Pressure buildup and CO_2 breakthrough time are found to be sensitive to storage-formation permeability and insensitive to all other hydrologic parameters that we investigated, with the exception of caprock-seal permeability, which only affects pressure buildup for cases with no brine production. Without brine production, brine leakage into the caprock can provide significant pressure relief; with brine production, the lack of sensitivity to caprock-seal permeability is indicative of minimal brine leakage.

Brine production from a horizontal well can strongly relieve pressure buildup at a horizontal CO_2 injector, which improves CO_2 injectivity. Pressure relief and injectivity improve with decreasing well spacing, while CO_2 breakthrough time is reduced. When injectors and producers are at the same depth in non-dipping formations, layered heterogeneity decreases CO_2 breakthrough time, while when brine is produced downdip of CO_2 injection, heterogeneity can delay CO_2 breakthrough. Injectivity ratio, which quantifies the improvement to injectivity caused by brine production, is insensitive to CO_2 injection rate, and is somewhat dependent on storage-formation thickness. The benefit of pressure relief is stronger for areally smaller storage formations than for larger formations. However, injectivity ratios were generally quite large (and always greater than 2), even if the storage formation is of infinite areal extent. Because an injectivity ratio greater than 2 decreases the total required number of wells, our results indicate that brine production may reduce well infrastructure costs.

The following are key findings from our reservoir study.

- **Pressure management without brine production** may require a combination of (1) CO_2-injection-rate reduction with time, (2) large storage-formation area, and (3) large spacing from adjacent CCS operations or other subsurface activities. If the storage formation is not large enough or neighboring subsurface operations are too close, this can constrain CO_2 injection rates and storage capacity.
- **Pressure management with brine production** may allow a large increase in CO_2 injectivity and storage capacity. CO_2 injection rate is not constrained by storage-formation area or by

Author's personal copy

proximity to neighboring CCS operations or other subsurface activities. Minimized pressure and fluid-migration interactions between neighboring CCS operations can help facilitate independent planning, assessment, and permitting of each CCS operation within a basin. Pressure relief increases with time, which allows the CO_2 injection rate to be continuously increased. Thus, additional CO_2 emitters could be continuously brought online.

- **Post-injection pressure buildup** persists long after injection ceases for CO_2 storage without brine production, while with brine production it abruptly drops to zero. With brine production, the only post-injection driving force is buoyancy, which is only strong enough to drive CO_2 updip, fully within the storage formation. Buoyancy is of much less concern (than pressure buildup) for diffuse leakage and for leakage up abandoned wells and permeable faults. With brine production, the driving force for post-injection brine migration can be eliminated. The difference in post-injection pressure buildup with and without brine production could affect post-injection monitoring requirements and the cost of liability insurance.
- **Control of CO_2-plume migration** with vertical brine producers may require too many wells to be practical, while for horizontal wells it appears to be quite promising, as it can counteract the influence of buoyancy.
- **Managing the tradeoff between pressure relief/injectivity improvement and delayed CO_2 breakthrough** appears to be feasible for both vertical and horizontal wells. The use of horizontal wells appears to be more promising with respect to improving injectivity and reducing the total number of wells.

The following are implications and recommendations derived from our study.

- **Consideration of brine utilization/disposition options** could play a role in the site selection process. The feasibility of various options for a particular site depends on the chemical composition and temperature of the produced brine, and proximity to potential markets. Of particular interest is whether salinity in the storage formation allows for cost-effective treatment, which is important to the economic feasibility of ACRM at sites where using brine as make-up water is not an option.
- **Greater selectivity in choosing CCS sites** may be enabled by ACRM. If sites are found where brine production and disposal is economically feasible, this may facilitate a large increase in injectivity and storage capacity, reducing the number of CCS sites required for a region, which allows greater selectivity in choosing sites. Larger storage capacity also enables greater leveraging of infrastructure costs, such as those associated with siting, permitting, and monitoring activities. We recommend consideration of the concept of "cherry picking", first searching for "upper echelon" sites where CCS may be deployed at reduced cost and risk.

In summary, ACRM provides benefits to reservoir management at the cost of extracting brine. This added cost must be offset by the added benefits to the storage operation and/or by creating new, valuable uses of brine that can reduce the added cost. The results from this study should motivate future, detailed studies of approaches and costs that will answer the question of the applicability of ACRM to specific CO_2 sequestration situations.

Acknowledgements

This work was sponsored by USDOE Fossil Energy, National Energy Technology Laboratory, managed by Andrea McNemar, and by the Carbon Mitigation Initiative at Princeton University and by the Environmental Protection Agency under Cooperative Agreement RD-83438501. The authors acknowledge the review of Pat Berge at Lawrence Livermore National Laboratory (LLNL). The authors also appreciate the comments from the reviewers, which helped this paper become a more thorough and comprehensive treatment of this subject. This work was performed under the auspices of the U.S. Department of Energy by LLNL under contract DE-AC52-07NA27344.

References

Aines, R.D., Wolery, T.J., Bourcier, W.L., Wolfe, T., Haussmann, C.W., 2011. Fresh water generation from aquifer-pressured carbon storage: feasibility of treating saline formation waters. Energy Procedia 4, 2269–2276.

Alhuthali, A.H., Oyerinde, D., Datta-Gupta, A., 2007. Optimal waterflood management using rate control. SPE Reservoir Evaluation & Engineering 10 (October (4)), 539–551, doi:10.2118/102478-PA.

ASME, 2006. ASME Steam Tables Compact Edition. ASME, Three Park Avenue, New York, NY, USA.

Bachu, S., 2008. CO_2 storage in geological media: role, means, status, and barriers to deployment. Progress in Energy and Combustion Science 34, 254–273.

Bergmo, P.E.S., Grimstad, A.-A., Lindberg, E., 2011. Simultaneous CO_2 injection and water production to optimize aquifer storage capacity. International Journal of Greenhouse Gas Control 5, 555–564.

Birkholzer, J.T., Zhou, Q., 2009. Basin-scale hydrogeologic impacts of CO_2 storage: capacity and regulatory implications. International Journal of Greenhouse Gas Control 3, 745–756.

Brouwer, D.R., Jansen, J.D., 2004. Dynamic optimization of water-flooding with smart wells using optimal control theory. SPEJ – Society of Petroleum Engineers Journal 9 (4), 391–402, doi:10.2118/78278-PA, SPE: 78278-PA.

Brouwer, D.R., Jansen, J.D., van der Starre, S., van Kruijsdkijk, C.P.J.W., Berentsen, C.W.J., 2001. Recovery increase through waterflooding with smart well technology. In: Paper SPE 68979 Presented at the SPE European Formation Damage Conference, The Haque, 21–22 May, doi:10.2118/68979-MS.

Bourcier, W.L., Wolery, T.J., Wolfe, T., Haussmann, C., Buscheck, T.A., Aines, R.D., 2011. A preliminary cost and engineering estimate for desalinating produced formation water associated with carbon dioxide capture and storage. International Journal of Greenhouse Gas Control 5, 1319–1328.

Breit, G.N., 2002. Produced Waters Database: U.S. Geological Survey Provisional Database, Available from: http://energy.cr.usgs.gov/prov/prodwat/index.htm.

Buscheck, T.A., Glascoe, L.G., Lee, K.H., Gansemer, J., Sun, Y., Mansoor, K., 2003. Validation of the multiscale thermohydrologic model used for analysis of a proposed repository at Yucca Mountain. Journal of Contaminant Hydrology 62 (3), 421–440.

Buscheck, T.A., 2010. Active management of integrated geothermal-CO_2-storage reservoirs in sedimentary formations: an approach to improve energy recovery and mitigate risk. In: Proposal in Response to DE_FOA-0000336: Energy Production with Innovative Methods of Geothermal Heat Recovery, LLNL-PROP-463758.

Buscheck, T.A., Sun, Y., Wolery, T.J., Court, B., Celia, M.A., Friedmann, S.J., Aines, R.D., 2011a. Active CO_2 reservoir management in saline formations: utilizing synergistic opportunities to increase storage capacity, reduce cost, and mitigate risk. In: Presentation at the SPE International Workshop on Carbon Capture, Utilization, and Storage (CCUS): Environment, Energy Security, and Opportunities for the Middle East, Abu Dhabi, UAE, 7–9 March.

Buscheck, T.A., Sun, Y., Hao, Y., Chen, M., Court, B., Celia, M.A., Wolery, T.J., 2011b. Geothermal energy production from actively-managed CO_2 storage in saline formations. In: Proceedings for the Geothermal Resources Council 35th Annual Meeting, San Diego, CA, USA, 23–26 October 2011.

Buscheck, T.A., Sun, Y., Hao, Y., Wolery, T.J., Bourcier, W.L., Tompson, A.F.B., Jones, E.D., Friedmann, S.J., Aines, R.D., 2011c. Combining brine extraction, desalination, and residual-brine reinjection with CO_2 storage in saline formations: implications for pressure management, capacity, and risk mitigation. Energy Procedia 4, 4283–4290.

Carroll, S., Hao, Y., Aines, R.D., 2008. Transport and detection of carbon dioxide in dilute aquifers. In: Proceedings for the 9th International Conference on Greenhouse Gas Control Technologies, Washington, DC, USA, 16–20 November 2008.

Carroll, S.A., Hao, Y., Aines, R.D., 2009. Geochemical detection of carbon dioxide in dilute aquifers. Geochemical Transactions 10, 4.

Court, B., 2011. Safety and Water Challenges in CCS: Modeling Studies to Quantify CO_2 and Brine Leakage Risk and Evaluate Promising Synergies for Active and Integrated Water Management, Ph.D. Dissertation, Princeton University, Princeton, NJ, available at http://ddspace.princeton.edu/jspui/handle/88435/dsp01ms35t861f.

Court, B., Elliot, T.R., Dammel, J., Buscheck, T.A., Rohmer, J., Celia, M.A., 2011a. Promising synergies to address water, sequestration, legal, and public acceptance issues associated with large-scale implementation of CO_2 sequestration, Special Issue on Carbon Capture and Storage (CCS) "Five years after the IPCC Special Report on CCS: state of play". Mitigation and Adaptation of Strategies for Global Change Journal, doi:10 1007/s11027-011-9314-x.

Author's personal copy

Court, B., Celia, M.A., Nordbotten, J.M., Elliot, T.R., 2011b. Active and integrated management of water resources throughout CO_2 capture and sequestration operations. Energy Procedia 4, 4221–4229.

Duke, D., 2007. ZLD: new silica based inhibitor chemistry permits cost effective water conservation for HVAC and industrial cooling towers. In: IWC Report 07-11, Proceedings for the 69th Annual International Water Conference, San Antonio, Texas, October 26–29, 2008.

Fenghour, A., Wakeham, W.A., Vesovic, V., 1998. The viscosity of carbon dioxide. Journal of Physical and Chemical Reference Data 27 (1), 31–44.

Harto, C.B., Veil, J.A., 2011. Management of Water Extracted from Carbon Sequestration Projects. Argonne National Laboratory, ANL/EVS/R-11/1.

Hassanzadeh, H., Pooladi-Darvish, M., Keith, D., 2009. Accelerating CO_2 dissolution in saline aquifers for geological storage: mechanistic and sensitivity studies. Energy and Fuels 23, 3328–3336.

IPCC (Intergovernmental Panel on Climate Change), 2005. IPCC Special Report on Carbon Dioxide Capture and Storage. Cambridge University Press, New York.

IEA International Energy Agency, 2007. Greenhouse Gas R&D Programme., http://www. ieagreen. org. uk/.

IEA International Energy Agency, 2009. How the energy sector can deliver on a climate agreement in Copenhagen. In: Special Early Excerpt of the World Energy Outlook 2009 for the Bangkok UNFCCC Meeting, http://www.iea.org/weo/docs/weo2009/climate_change_excerpt.pdf.

Johnson, J.W., Nitao, J.J., Knauss, K.G., 2004a. Reactive transport modeling of CO_2 storage in saline aquifers to elucidate fundamental processes, trapping mechanisms and sequestration partitioning. In: Baines, S.J., Worden, R.H. (Eds.), Geological Storage of Carbon Dioxide. Special Publications, vol. 223. Geological Society, London, pp. 107–128.

Johnson, J.W., Nitao, J.J., Morris, J.P., 2004b. Reactive transport modeling of cap rock integrity during natural and engineered CO_2 storage. In: Benson, S. (Ed.), CO_2 Capture Project Summary, vol. 2. Elsevier.

Keith, D., Hassanzadeh, H., Pooladi-Darvish, M., 2004. Reservoir engineering to accelerate dissolution of stored CO_2 in brines. In: Gale, J., Wilson, M. (Eds.), Proceedings for the 7th International Conference on Greenhouse Gas Control Technologies. Elsevier.

Maulbetsch, J.S., DiFilippo, M.N., 2010. Performance, cost, and environmental effects of saltwater cooling towers. In: California Energy Commission, PIER Energy-Related Environmental Research Program. CEC-500-2008-043, http://www.energy.ca.gov/2008publications/CEC-500-2008-043/CEC-500-2008-043.pdf.

MIT, 2006. The Future of Geothermal Energy: Impact of Enhanced Geothermal Energy Systems (EGS) in the United States in the 21st Century., http://www1.eere.energy.gov/geothermal/egs_technology.html.

Morris, J.P., Detwiler, R.L., Friedmann, S.J., Vorobiev, O.Y., Hao, Y., 2011. The large-scale geomechanical and hydrological effects of multiple CO_2 injection sites on formation stability. International Journal of Greenhouse Gas Control 5, 69–74.

Nitao, J.J., 1998. Reference Manual for the NUFT Flow and Transport Code, Version 3.0. Lawrence Livermore National Laboratory, UCRL-MA-130651-REV-1.

Rutqvist, J., Birkholzer, J., Cappa, F., Tsang, C.-F., 2007. Estimating maximum sustainable injection pressure during geological sequestration of CO_2 using coupled fluid flow and geomechanical fault-slip analysis. Energy Conversion and Management 48, 1798–1807.

Sanz, M.A., Stover, R.L., 2007. Low energy consumption in the Perth seawater desalination plant. In: Presented at IDA World Congress, Maspalomas, Gran Canaria, Spain, 21–26, 2007.

Span, R., Wagner, W., 1996. A new equation of state for carbon dioxide covering the fluid region from the triple-point temperature to 1100 K at pressures up to 800 MPa. Journal of Physical and Chemical Reference Data 25, 1509–1596.

Sudaryanto, B., Yortsos, Y.C., 2001. Optimization of displacements in porous media using rate control. In: Paper SPE 71509 Presented at the SPE Annual Technical Conference and Exhibition, New Orleans, 30 September–3 October, doi:10.2118/71509-MS.

Surdam, R.C., Jiao, Z., Stauffer, P., Miller, T., 2009. An Integrated Strategy for Carbon Management Combining Geological CO_2 Sequestration, Displaced Fluid Production and Water Treatment. Wyoming State Geological Survey, Challenges in Geologic Resource Development No. 8.

van Genuchten, M.T., 1980. A closed form equation for predicting the hydraulic conductivity of unsaturated soils. Soil Science Society of America Journal 44, 892–898.

Veil, J.A., Puder, M.G., Elcock, D., Redwick Jr., R.J., 2004. A White Paper Describing Produced Water from Production of Crude Oil, Natural Gas, and Coal Bed Methane. US DOE National Energy Technology Laboratory Report, http://www.evs.anl.gov/pub/doc/ProducedWatersWP0401.pdf.

Zhou, Q., Birkholzer, J.T., Tsang, C.-F., Rutqvist, J.A., 2008. A method for quick assessment of CO_2 storage capacity in closed and semi-closed saline formations. International Journal of Greenhouse Gas Control 2, 626–639.